International Journal of Biological Macromolecules 255 (2024) 128087

Contents lists available at ScienceDirect

International Journal of Biological Macromolecules

journal homepage: www.elsevier.com/locate/ijbiomac

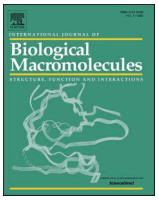

Sustained drug release behavior of captopril-incorporated chitosan/carboxymethyl cellulose biomaterials for antihypertensive therapy

Kyeong-Jung Kim [a,1], Min-Jin Hwang [b,e,1], Wang-Geun Shim [c,1], Young-Nam Youn [d,*], Soon-Do Yoon [a,*]

[a] Department of Chemical and Biomolecular Engineering, Chonnam National University, Yeosu 59626, Republic of Korea
[b] Department of Environmental System Engineering, Chonnam National University, Yeosu 59626, Republic of Korea
[c] Department of Chemical Engineering, Sunchon National University, Suncheon, Jeollanam-do 57922, Republic of Korea
[d] Division of Cardiovascular Surgery, Severance Cardiovascular Hospital, YONSEI University College of Medicine, Seoul 03722, Republic of Korea
[e] Smart Plant Reliability Center, Chonnam National University, Yeosu 59626, Republic of Korea

ARTICLE INFO

Keywords:
Chitosan/carboxymethyl cellulose biomaterials
Captopril
Release behavior
Angiotensin-converting enzyme inhibitory activity

ABSTRACT

Captopril (CTP) is an oral drug widely used to treat high blood pressure and congestive heart failure. In this study, CTP-incorporated biomaterials for antihypertensive therapy were synthesized from chitosan, carboxymethyl cellulose, and plasticizers. The physicochemical properties of the prepared biomaterials were characterized using FE-SEM, FT-IR analysis, and physical properties. CTP release experiments were carried out in buffer solutions at various pH values and temperatures. Results indicated that above 99.0 % of CTP was released within 180 min. Optimization of the experimental conditions for CTP release was analyzed by using response surface methodology (RSM). Results of CTP release through artificial skin indicated that CTP was continuously released above 95.0 % from the prepared biomaterials for 36.0 h. The CTP release mechanisms into a buffer and through artificial skin followed pseudo-Fickian diffusion mechanism and non-Fickian diffusion mechanisms, respectively. Moreover, angiotensin-converting enzyme (ACE) inhibition (related to cardiovascular disease) via the released CTP clearly reveals that the prepared biomaterials have a high potential as a transdermal drug delivery agent in antihypertensive therapy.

1. Introduction

Oral administration is the most common route for drug delivery systems and is preferred by many patients because it is non-invasive. However, drugs delivered by this route are affected by the first-pass metabolism and gastrointestinal environment, resulting in reduced bioavailability [1,2]. Therefore, delivering the drug using another route is necessary to overcome the reduced therapeutic effect of the drug. A transdermal drug delivery system (TDDS) is a non-invasive method of delivering an effective amount of a drug through the patient's skin. In particular, it can avoid degradation of the drug in the gastrointestinal tract and the first pass in the liver that occurs with oral administration, thereby improving the bioavailability of the drug and reducing its side effects. In addition, it has advantages such as sustained drug release, less frequent dosing, and improved patient compliance [3–5]. The demand for TDDS as drug carriers is rising due to the increasing number of patients with chronic diseases and the convenience of self-administration. Moreover, it is estimated that the global market for them will grow gradually and reach a value of approximately $95.57 billion by 2025 [6].

Hypertension is a chronic condition that is a significant cause of cardiovascular disease. It is characterized by the pressure in the blood vessels being continuously high, with systolic and diastolic pressures of ≥140 and ≥90 mm Hg, respectively. Globally, hypertensive patients were estimated to be around 1.4 billion in 2010, which is predicted to exceed 1.6 billion by 2025. In 2016, 44 % of non-communicable disease-related deaths were from cardiovascular disease with hypertension as a major risk factor. These statistics indicate the severity of hypertension both currently and in the future [7–9]. Furthermore, because blood pressure generally increases with age, the prevalence of hypertension and the utilization of antihypertensive drugs at high-dose for its treatment have been predicted to grow with increasing life expectancy [10].

* Corresponding authors.
E-mail addresses: ynyoun@yuhs.ac (Y.-N. Youn), yunsd03@jnu.ac.kr (S.-D. Yoon).
[1] These authors contributed equally to this work.

https://doi.org/10.1016/j.ijbiomac.2023.128087
Received 3 July 2023; Received in revised form 21 October 2023; Accepted 12 November 2023
Available online 17 November 2023

Captopril (CTP) is an angiotensin-converting enzyme (ACE) inhibitor and is an oral drug widely used in the treatment of hypertension and congestive heart failure [11]. ACE is an enzyme that not only converts angiotensin I to a potent vasoconstrictor peptide angiotensin II but also mediates the inactivation of a vasoactive peptide. Clearly, since ACE plays an important role in the blood pressure-increasing mechanism, using CTP as an ACE inhibitor is effective in the treatment of hypertension [12–14]. Orally administered CTP must be at a high dose because it has a relatively short half-life in the plasma, an absorption rate of 70–75 %, and a bioavailability of 65 %. It has been reported that changes in gastric pH due to food intake can reduce its bioavailability by 35–55 % [15,16]. Many studies have reported the preparation of functional biomaterials containing CTP as the drug and the evaluation of physicochemical properties and drug release behavior using 'in vitro' and 'in vivo' studies [17–19]. However, CTP can cause some side effects such as sleep and taste disturbances, dizziness, persistent coughing, gastrointestinal discomfort, and rashes [20,21]. Therefore, developing a CTP-incorporated TDDS for reducing these side effects and increasing bioavailability is essential.

Chitosan (CS) is an FDA-approved copolymer consisting of glucosamine and *N*-acetyl glucosamine unit linked by 1, 4-glucosidic bonds produced by deacetylating chitin extracted from arthropod shells. It is biologically active, biocompatible, and non-toxicity with both antimicrobial properties and hemostatic properties. In addition, it can be modified into various forms depending on the application. Amine groups in the CS backbone are uniquely protonated at acidic pH, which can be exploited to form complexes by interacting with anionic polymers. Based on these properties, CS-based complexes have been used in several biomedical fields such as drug delivery, hemostatic wound dressings, and tissue engineering scaffolds [22,23].

Carboxymethyl cellulose (CMC) is a modified cellulose obtained by the carboxymethylation of cellulose that is used as a food additive [24]. Because it is an anionic polymer, electrostatic interaction between the carboxyl groups in CMC and the amine groups in CS can easily form complexes that have been used for drug delivery. Because CMC have good biological stability, biocompatibility, and gel formation, they have been applied as oral formulations, either individually or in complexes [25]. In addition, various attempts have been made to prepare complexes using chelation of CMC for anticancer, antioxidant, and drug delivery. Lotfy et al. conjugated various amino acids with CMC to form complexes with Pd(ii) ions to evaluate the proliferation inhibition of colon cancer cells and DPPH radical scavenging activities, and Basta et al. reported antibacterial and anticancer activities of CMC-Ag(I) complexes [26,27]. In the agricultural, control of fertilizer release and improved nutrient content of onions have been reported by loading monoammonium phosphate into a complex of Cu(II) or trimethyl chitosan and CMC [28]. Moisture-sensitive CMC can also be used in edible films by forming complexes with gelatin and adding essential oils to increase antibacterial properties and reduce water vapor permeability. In the field of bone tissue engineering, the combination of CMC with nano-hydroxyapatite/CS complexes and in vivo implantation of these composites has been used for bone scaffolds. Besides, CMC are applied in cosmetics, paper industry, textiles industry, wound healing, etc. [29–33].

Biomaterials used for TDDS must be non-toxic, non-carcinogenic, and antibacterial. They include biodegradable synthetic polymers (e.g., poly(vinyl alcohol), polyacrylamide, poly(ethylene glycol), polylactides, poly(lactide-co-glycolide), and poly(butylene adipate-*co*-terephthalate)), proteins (e.g., albumin, collagen, casein, gelatin, silk, and zein), and natural polymers (e.g., starch, alginate, chitosan, cellulose, heparin, and pullulan). Although biomaterials using natural polymers derived from plants and animals provide better biodegradability and biocompatibility than biodegradable synthetic polymers [34], their usually poor physical properties make it difficult to completely replace biodegradable synthetic polymers. Nevertheless, crosslinking methods using a plasticizer or crosslinking agent, UV irradiation, heat treatment, etc. can improve the physical properties of natural polymer-based biomaterials and expand their applicability [35].

Table 1
Composition of CTP-incorporated chitosan/CMC biomaterials.

Sample name	CS[a] (g)	CMC[b] (g)	CA[c] (wt%)	GL[d] (wt%)	CTP[e] (g)	DW[f] (g)
CS/CMC	2.0	2.0	–	–	–	400
CS/CMCCTP	2.0	2.0	–	–	0.5	400
CS/CMCCA4	2.0	2.0	40	–	–	400
CS/CMCCA4CTP	2.0	2.0	40	–	0.5	400
CS/CMCGL4	2.0	2.0	–	40	–	400
CS/CMCGL4CTP	2.0	2.0	–	40	0.5	400

[a] Medium molecular weight chitosan.
[b] Carboxymethyl cellulose.
[c] Citric acid.
[d] Glycerol.
[e] Captopril.
[f] Distilled deionized water.

In this study, CTP-incorporated biomaterials were prepared using CS/CMC complexes and plasticizers (citric acid (CA) and glycerol (GL)) followed by UV irradiation. Many studies have reported the development of transdermal drug delivery patches for antihypertensive therapy [36,37]. However, there have been few studies using eco-friendly biodegradable materials and press needles (PN) which were commonly used in oriental medicine to effectively deliver drugs intradermally. To determine the optimal UV irradiation time for the preparation of CTP-incorporated biomaterials, the water resistance properties of the prepared CS/CMC biomaterials after various UV irradiation times were investigated. CTP release properties of CTP-incorporated CS/CMC biomaterials for antihypertensive treatment were evaluated. To determine their applicability in a TDDS, their CTP release properties were confirmed via an artificial skin test and the CTP release mechanism was investigated using kinetic models of Fickian diffusion and Korsmeyer-Peppas models. Moreover, CTP-incorporated CS/CMC biomaterials were prepared with PN to controlled release of CTP. To assess the enhanced drug delivery and potential controlled release of the prepared PN combined biomaterials, the CTP release properties were confirmed in artificial skin tests. Finally, their ACE inhibitory activity was investigated.

2. Experimental

2.1. Materials

The medium molecular weight chitosan (CS) (Mw: 190,000–310,000 and the degree of deacetylation: 75–85 %), sodium carboxymethyl cellulose (CMC) (average Mw: 250,000 and degree of substitution: 0.7), captopril (CTP), glycerol (GL), citric acid (CA), lactic acid, boric acid, sodium chloride (NaCl), hydrochloric acid (HCl), angiotensin-converting enzyme (ACE) from rabbit lung, N-hippuryl-His-Leu hydrate (HHL), and ethyl acetate (EA) were obtained from Sigma-Aldrich (St. Louis, MO, USA). Standard buffer solutions (pH = 4.01 and pH = 7.0) were purchased from Duksan (Pharmaceutical Co., Ltd., Korea). Press needles (PN) were obtained from Dongbang Medical (South Korea). Distilled deionized water (DW) was used in all of the experiments.

2.2. Preparation of CTP-incorporated CS/CMC biomaterials

CTP-incorporated CS/CMC biomaterials were obtained by a sample casting method. First, CS solution was prepared by dissolving CS in the aqueous solution of lactic acid of 1 wt% at room temperature. After preparing CMC solution (1.0 %) using DW, CTP and plasticizers (CA and GL) were mixed in a CMC solution. The CMC/CTP/plasticizers mixed solution was subsequently added dropwise to the CS solution, followed

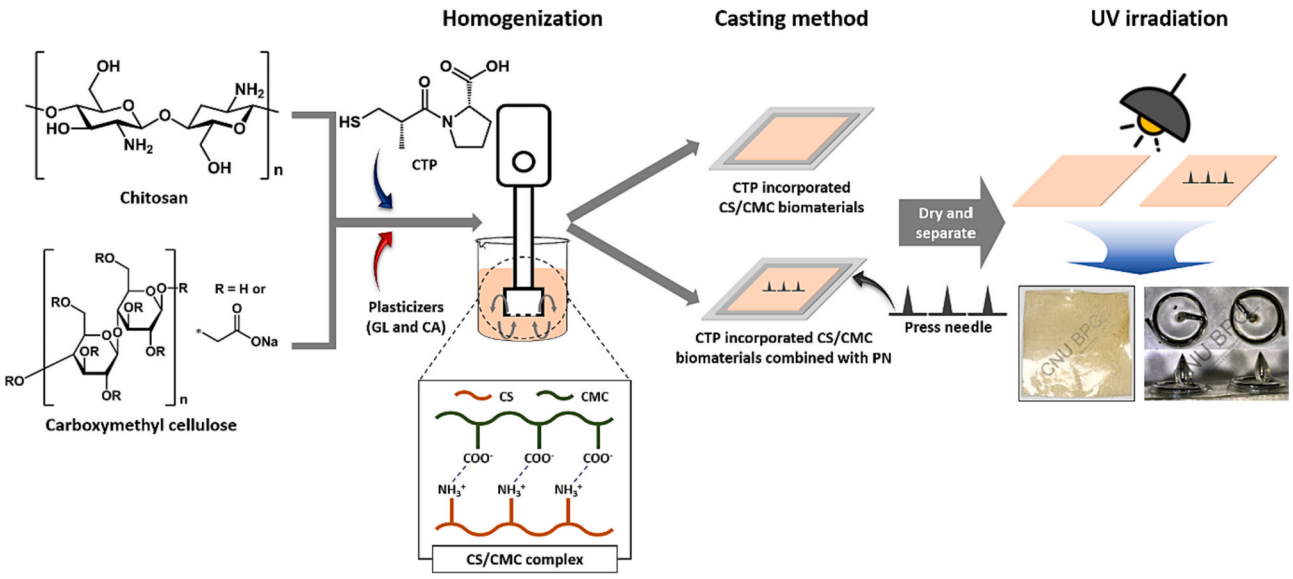

Scheme 1. Flowchart for preparation of CTP-incorporated CS/CMC biomaterials.

by homogenized at 30,000 rpm for 5 min using a homogenizer (Ingenieurbüro CAT M. Zipperer GmbH, Antrieb × 120, Germany). CS and CMC had the same ratio, and biomaterials contained plasticizers equivalent to 40 wt% of the total weight of CS and CMC. The constituents in the CTP-incorporated CS/CMC biomaterials with/without the addition of plasticizers are summarized in Table 1. Afterward, the homogeneous CS/CMC complex solution was poured into a preheated Teflon mold (50.0 °C, 250 × 250 × 1 mm). Then, Water in the Teflon mold was evaporated in a ventilated oven at 50 °C for 24 h. The prepared CS/CMC biomaterials were irradiated for 10 to 60 min under an atmospheric pressure UV lamp (OSRAM ULTRA VITALUX, 300 W) [38]. In addition, CTP-incorporated CS/CMC biomaterials combined with PN were prepared as follows: After the casting process of a gel-like solution, functional biomaterials were synthesized by adding PN before drying these biomaterials. The preparation process of CS/CMC biomaterials is explained in Scheme 1.

2.3. Characterization

The water uptake (WU) and solubility (S) were investigated to evaluate the water resistance properties of the CS/CMC biomaterials. The dried biomaterial pieces (ca. 0.1 g) were immersed in DW (30 mL) at 25 °C. After 24 h, which was when equilibrium had been reached, the moisture on the surface of the biomaterials was removed, and the weights of the biomaterials were measured. The WU of biomaterials was calculated as follows (Eq. (1)):

$$\text{Water uptake (WU)} = \frac{W_e - W_0}{W_0} \quad (1)$$

where W_e is the weight of the swelling biomaterials at equilibrium, and W_0 is the initial weight of the dried biomaterials.

The swollen biomaterials were dried again at 50.0 °C for 24 h, after which its S was calculated as follows (Eq. (2)):

$$\text{Solubility (S)} = \frac{W_0 - W_d}{W_d} \quad (2)$$

where W_d is the dry weight of the swollen biomaterials and W_0 is the initial weight of the dried biomaterials.

The tensile strength (TS) and elongation at break (EB) of the prepared CS/CMC biomaterials were investigated by using an Instron 6012 testing machine (Norwood, MA, USA). Six dumbbell-shaped specimens with a width of 15.0 mm (ASTM D-421) were cut from each biomaterial. The thickness of specimens was measured at three places along the test length using a Mitutoyo digital thickness gauge (Tokyo, Japan) at 12 random positions around biomaterials. The average thickness of the specimens was 0.131 ± 0.005 mm. The gauge length and grip distance were both 53.0 mm. The crosshead speed was 20 mm/min, and the load cell was 250 kg_f. The tests were performed at 25 °C under 55.0 % RH.

The morphologies of both pristine and UV irradiated CS/CMC biomaterials were observed by using field emission scanning electron microscopy (FE-SEM, ZEISS Sigma 500, Carl Zeiss Co., Ltd., Germany) at an accelerating voltage of 5.0 kV. Fourier transform infrared (FT-IR) spectroscopy of CTP and prepared biomaterials was performed using an FT-IR spectrophotometer (Spectrum Two, Perkin Elmer, USA). To evaluate the stability of UV irradiated CTP, UV absorbance curves of CTP solutions were analyzed using a UV–vis spectrophotometer (OPTIZEN 2120UV, Neogen, Co., Ltd., Korea). In addition, CTP before and after UV irradiation was analyzed using ^{1}H nuclear magnetic resonance (^{1}H NMR) spectra. ^{1}H NMR was recorded on a Varian Unity Inova 500 MHz spectrometer at the Korea Basic Science Institute (KBSI, Gwangju Center, Korea). Samples were dissolved in $CDCl_3$.

Thermogravimetric analysis (TGA) and differential scanning calorimetry (DSC) of CS/CMC biomaterials were performed using a DSC Q200/TGA Q50 (TA Instruments, USA) in an N_2 environment (flow rate: 20 mL/min). TGA and DSC were conducted at 25 °C to 600 °C and 25 °C to 500 °C, respectively, at a heating rate of 10 °C/min. The sample weight was between 10.0 and 11.0 mg.

2.4. CTP release testing

The CTP release of CTP-incorporated CS/CMC biomaterials with/without the addition of plasticizers was performed in buffers with various pH values (pH 4.5, 5.5, and 6.5) and temperatures (32.0, 36.5, and 40.0 °C). pH buffer solutions were prepared using acetate (pH 4.0–5.5) and phosphate (pH 6.0–7.5) buffer solutions, respectively. The prepared biomaterials (0.1 g) were immersed in 30 mL buffer, followed by incubating in a shaking incubator (VS-8480SF, Vision, Scientific Co., Korea) at 50 rpm. At appropriate time intervals, the release medium was withdrawn and the concentration of CTP was measured using a UV–vis spectrophotometer at 200 nm. The cumulative drug release was calculated using a standard calibration curve. The application of TDDS to the CTP-incorporated CS/CMC biomaterials was also evaluated via an artificial skin test (Neoderm-ED, Tego Science, Inc. Korea). The prepared biomaterials (ca. 2.0 × 2.0 cm) were applied to artificial skin fixed in a

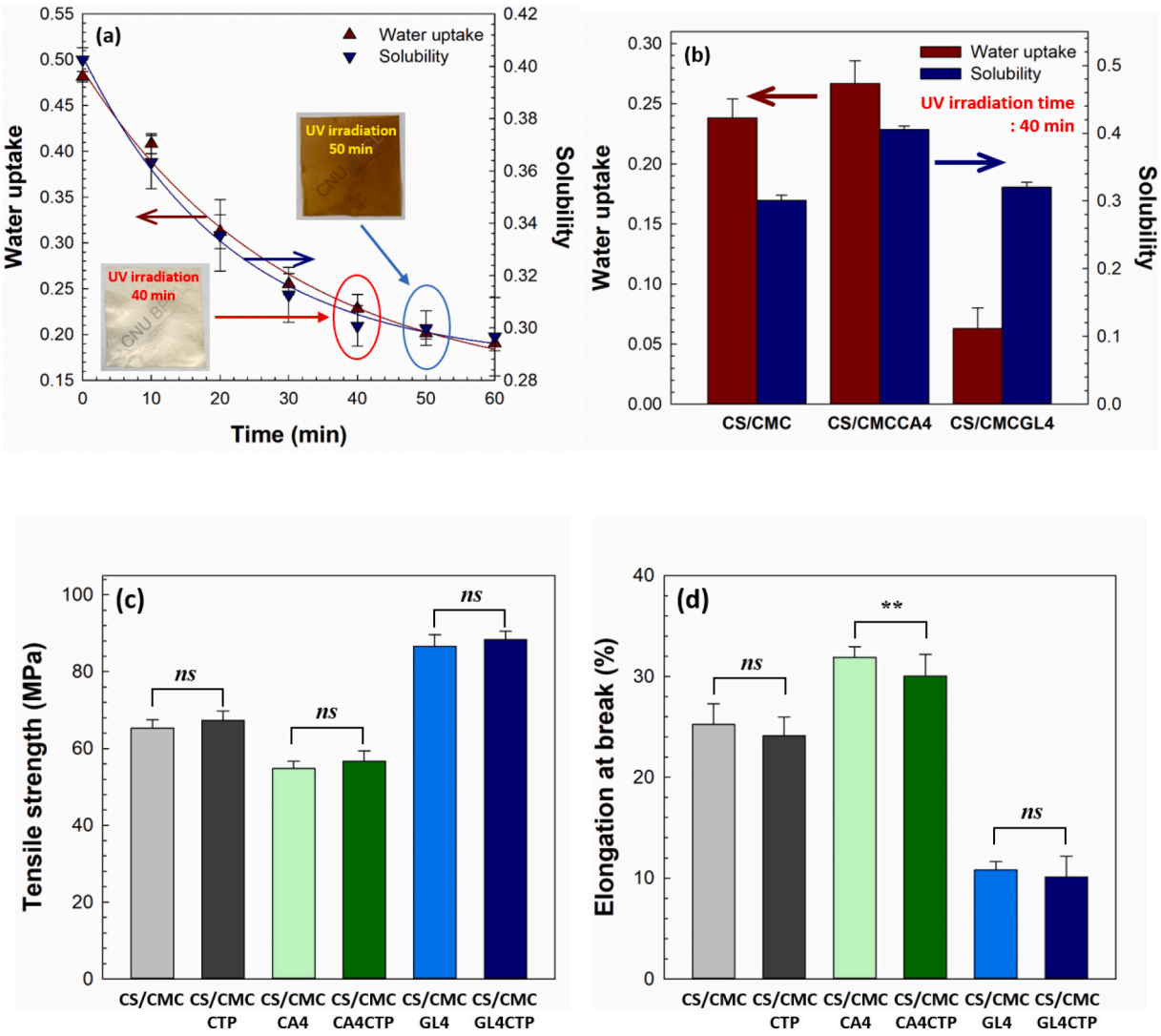

Fig. 1. Physical properties of CS/CMC biomaterials. (a) Water uptake (WU) and solubility (S) of CS/CMC biomaterials with UV irradiation time. (b) WU and S of CS/CMC biomaterials with/without plasticizer under UV irradiation for 40 min. (c) Tensile strength (MPa) and elongation at break (%) of CS/CMC biomaterials with/without CTP and plasticizers under UV irradiation for 40 min ($N = 6$ each, ** < 0.01, and ns > 0.05). (d) Elongation at break (%) of CS/CMC biomaterials with/without CTP and plasticizers under UV irradiation for 40 min ($N = 6$ each, ** < 0.01, and ns > 0.05).

medium containing agarose at RH 60.0 % and 36.5 °C. Subsequently, the released biomaterials were removed from the artificial skin for a predetermined time, and the medium of the artificial skin was separated. This medium was immersed in DW and left for 8 h at room temperature. The quantities of CTP released from the biomaterials in this mixture were measured using UV–vis spectrophotometry. The release properties of CTP in CTP-incorporated CS/CMC biomaterials with/without the addition of PN were further tested on artificial skin using the same method.

2.5. CTP release mechanism

Drug release signifies that the drug migrates from the initial location in the biomaterial to the outside, then makes contact with and is consequently released into the medium. Furthermore, elucidating the diffusion mechanism of these drugs enables the systematic evaluation of the release kinetics in the polymer matrix. We verified the CTP release kinetics using the Fickian diffusion and Korsmeyer-Peppas models.

Fick's law is used to determine the diffusion coefficient of a drug released from biomaterials (Eq. (3)) [39,40].

$$\frac{\partial C}{\partial t} = D\frac{\partial^2 C}{\partial x^2} \tag{3}$$

where C is the concentration at time t and D is the constant diffusion coefficient. In the thin polymer slab, the solution of Eq. (3) can be rearranged in the form of a trigonometric series and can be expressed as Eq. (4), which is known as the Fickian diffusion model.

$$\frac{M_t}{M_\infty} = 1 - \sum_{n=0}^{\infty} \frac{8}{(2n+1)^2 \bullet \pi^2} exp\left[-\frac{D_{eff} \bullet (2n+1)^2 \pi^2}{l^2} t\right] \tag{4}$$

where M_t and M_∞ are the amounts of drug released from the biomaterial at diffusion time and infinite time, respectively; l is the half thickness of the biomaterial; D_{eff} is the diffusion coefficient.

The Korsmeyer-Peppas model can be defined as the following equation (Eq. (5)) [41]:

$$\frac{M_t}{M_\infty} = kt^n \tag{5}$$

where k is the drug release constant and n is the diffusional exponent, indicative of the mechanism of drug release. $n < 0.5$ indicates that the

release behavior is a pseudo-Fickian diffusion mechanism, $n = 0.5$ implies a Fickian diffusion mechanism, and $0.5 > n > 1.0$ infers a non-Fickian diffusion mechanism [42,43].

2.6. Optimizing CTP release from CTP-incorporated biomaterials

The experimental design for this was based on the response surface methodology (RSM) method reported by Brahima et al. [44] and Lee et al. [45]. To examine the CTP release behavior at various pH values (4.5, 5.5, and 6.5) and temperatures (32.0, 36.5, and 40.0 °C), the response for CTP release was calculated using the following functions (Eq. (6)).

$$P = \beta_0 + \beta_1 Q_1 + \beta_2 Q_2 + \beta_{12} Q_1 Q_2 + \beta_{11} Q_1^2 + \beta_{22} Q_2^2 + \ldots$$
$$P = \beta_0 + \sum_{i=1}^{k} \beta_i Q_i + \sum_{i<j}^{K} \beta_{ij} Q_i Q_j + \sum_{i=1}^{k} \beta_{ii} Q_i^2 + \ldots \quad (6)$$

where P is the response for CTP release, Q represents the design variables (pH, temperature, and time) and β represents the model coefficients.

2.7. ACE inhibitory activity of the CTP-incorporated CS/CMC biomaterials

ACE inhibitory activity of prepared CTP-incorporated CS/CMC biomaterials was conducted using a previously reported method based on the release of hippuric acid (HA) from HHL using the ACE as the catalyst [46]. First, sodium borate buffer solution was prepared using boric acid and 0.3 M NaCl (pH 8.3). 0.3 mL of 10 mM HHL in 100 mM sodium borate buffer containing 0.3 M NaCl (pH 8.3) was mixed with 0.3 mL released solution of prepared biomaterials. Subsequently, 0.1 mL of 4.0 mU ACE in sodium borate buffer was added and incubated at 36.5 °C, after which the reaction was stopped by the addition of 0.2 mL of 1.0 M HCl. Next, 1.0 mL of EA was added to the reaction mixture, which was then centrifuged at 3000 rpm for 5 min to extract the produced HA, Afterward, 0.7 mL of the upper organic layer of these solutions was collected and completely evaporated off by heating at 80 °C for 40 min in a 5 mL glass vial. The dried biomaterial was then dissolved in 2 mL DW and the absorbance was analyzed via UV–vis spectroscopy at 228 nm. The degree of ACE inhibition (%) was calculated as follows (Eq. (7)):

$$\text{ACE inhibition } (\%) = \left(1 - \frac{B - C}{A - D}\right) \times 100 \quad (7)$$

where A is the absorbance in the presence of ACE, B is the absorbance in the presence of ACE and the released solution, C is the absorbance by the reaction stopping blank in the presence of the released solution, and D is the absorbance by the reaction stopping blank. For A and D, the buffer was used instead of the released solution.

2.8. Statistical analysis

In all test, Statistical analyses were performed using SPSS statistical software for Windows version 25.0 (IBM). In addition, data distribution was ascertained via Student's t-tests. A p-value <0.05 was considered statistically significant and all results are represented as mean ± standard deviation (SD).

3. Results and discussion

3.1. Characterization of CS/CMC biomaterials

Evaluation of the mechanical and water resistance properties of eco-friendly biodegradable materials or biomaterials plays an important role in their applicability in various fields (e.g., biomedical engineering, chemical engineering, biological engineering, etc.). Especially, water resistance properties such as water uptake (WU) and solubility (S) are

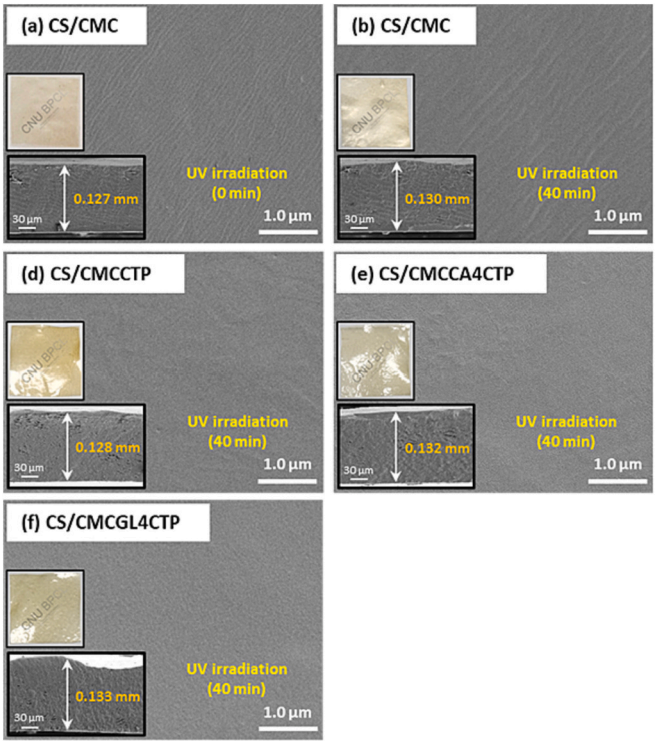

Fig. 2. FE-SEM images of surfaces and cross-sections of CS/CMC biomaterials. (a) CS/CMC biomaterials. (b) CS/CMC biomaterials with UV irradiation. (c) CTP-incorporated CS/CMC biomaterials. (d) CTP-incorporated CS/CMC biomaterials with UV irradiation. (e) CTP-incorporated CS/CMC biomaterials with CA and UV irradiation. (f) CTP-incorporated CS/CMC biomaterials with GL and UV irradiation.

criteria that can be used to evaluate the degree of crosslinking in biomaterials.

Fig. 1a shows the results of WU and S of CS/CMC biomaterials with increasing UV irradiation time; both decreased drastically until 40 min and then decreased slightly when the UV irradiation time exceeded 40 min. The reason for this is the degree of crosslinking between the components in the CS/CMC biomaterials was enhanced by the UV curing process. Conversely, with a long UV irradiation time of over 40 min, the decreases in their WU and S were due to the dissolution of the cross-linked short-length molecules or polymer chains [47]. Moreover, the samples turned yellow and oxidation occurred therein. Hence, the optimal UV irradiation time was set as 40 min. Fig. 1b shows the WU and S of CS/CMC biomaterials with the addition of plasticizers (CA and GL). Results indicated that the WU of GL-added biomaterial (CS/CMCGL4) was lower than those of the biomaterial without the addition of plasticizers (CS/CMC) and CA-added biomaterial (CS/CMCCA4). The reason is attributed to the strong hydrogen bonding of the hydroxyl groups contained in GL, which improves intermolecular interactions. In addition, the WU and S of CS/CMCCA4 were higher than those of the other biomaterials. When CS and CMC form a complex, the augmentation of amine groups enhances the electrostatic interaction with carboxyl groups. However, due to the addition of carboxyl groups in CA, the amine groups in the complex were relatively reduced, which is considered to weaken the interaction between CS and CMC [48]. Thus, the water resistance properties of the biomaterial were reduced by the addition of CA. In addition, it is considered that because unreacted CA has high hydrophilic properties was dissolved in DW.

The mechanical properties such as TS and EB of CS/CMC biomaterials with/without loading CTP and/or plasticizers are shown in Fig. 1c and d. Results indicated that GL-added biomaterials had higher TS and lower EB than the others. Contrastively, the EB of CA-added

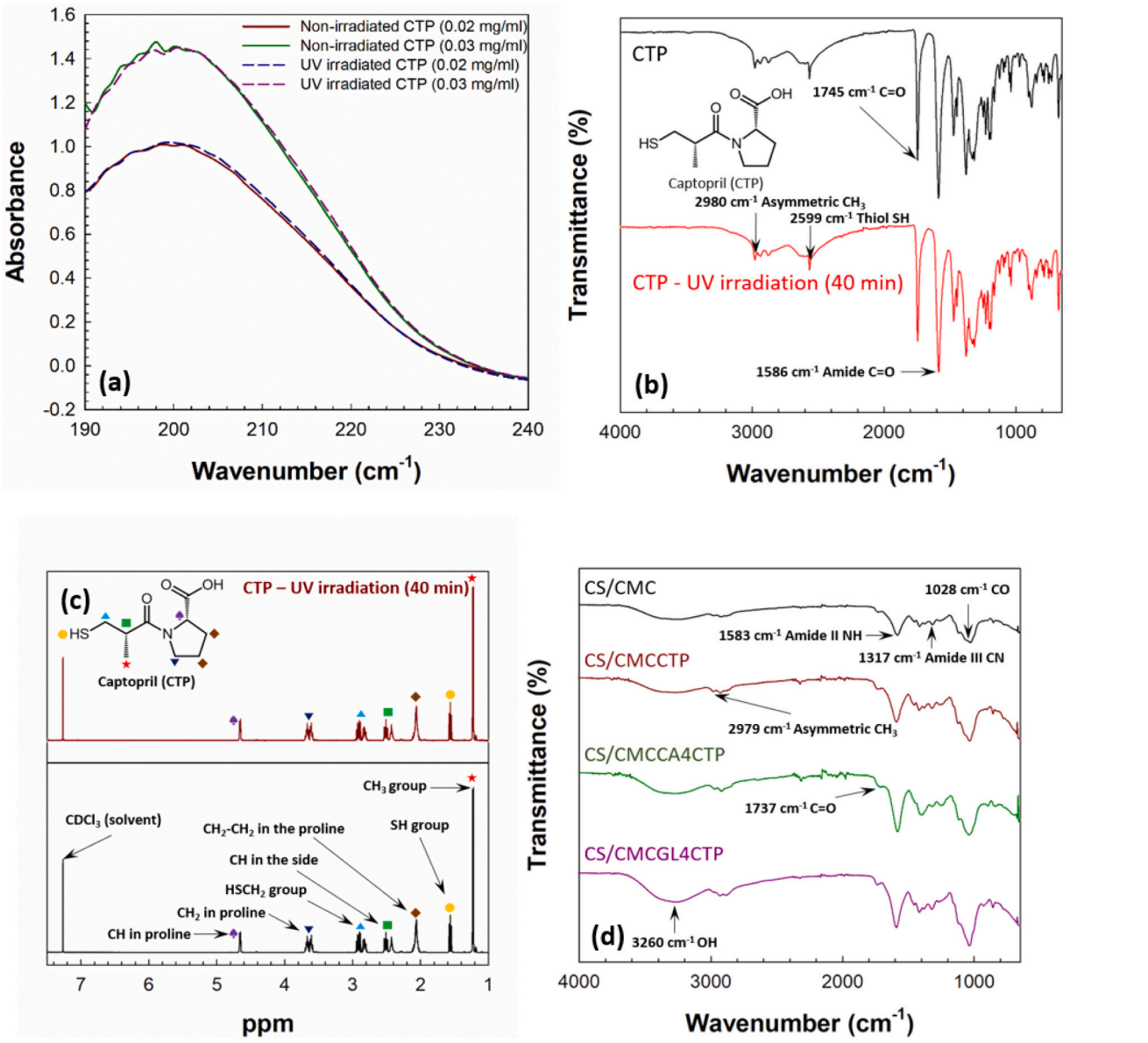

Fig. 3. (a) UV absorbance curves of CTP solution with/without UV irradiation. (b) FT-IR spectra of CTP with/without UV irradiation. (c) ^{1}H NMR spectra of CTP with/without UV irradiation (d) FT-IR spectra of CS/CMC biomaterials with/without the addition of CTP and plasticizers.

biomaterials increased whereas the TS decreased. These variations in mechanical properties for prepared biomaterials infer that the functional groups in the plasticizers caused changes in the intermolecular interactions between CS/CMC biomaterials. In addition, there is no significant difference in these mechanical properties of prepared biomaterials with/without the addition of CTP.

SEM images of the surfaces and cross-sections of the prepared CS/CMC biomaterials with/without the addition of plasticizers are shown in Fig. 2. It can be seen that they had homogeneous surfaces without noticeable porosity, flaws, or cracks that were unaffected by the UV curing process.

UV–vis spectrophotometry, FT-IR, and ^{1}H NMR analyses were performed to evaluate the deformation and stability of CTP by UV irradiation. The UV absorbance curves of CTP solutions at various concentrations before/after UV irradiation in Fig. 3a show that the characteristic peak for CTP was unaffected by UV absorbance. The FT-IR spectra of CTP before/after UV irradiation for 40 min in Fig. 3b revealed at 2980 cm^{-1} for asymmetric CH_3 and 2599 cm^{-1} for the S—H stretching vibration in the thiol groups. Sharp peaks at 1745 and 1586 cm^{-1} correspond to the C═O vibrations of carboxylic acid and amide groups, respectively [49,50]. These results indicate that UV irradiation of CTP did not change its structure. ^{1}H NMR analysis of CTP before/after UV irradiation uncovered specific peaks for CTP at 1.22, 1.58, 2.06, 2.48, 2.88, 3.67, and 4.66 ppm for protons (Fig. 3c) [51]. Results indicated that CTP was not photolyzed by UV irradiation at the preparation condition of biomaterials. FT-IR spectra of prepared CS/CMC biomaterials with/without the addition of CTP or plasticizers in Fig. 3d indicate N—H bending of amide II at 1583 cm^{-1}, C—N stretching in amide III at 1317 cm^{-1}, and C—O stretching at 1060 cm^{-1} [38,52]. In addition, the spectra of the GL-added CS/CMC biomaterials contained a broad peak at 3260 cm^{-1}, which was attributed to the hydroxyl groups of GL. Meanwhile, all of the FT-IR spectra of CTP-incorporated biomaterials with/without plasticizers (CA or GL) showed characteristic peaks for CTP at 1745.0 and 1586.0 cm^{-1}. However, other specific peaks for CTP could not be identified because of overlapping with the related transitions of the chemical structures of the biomaterial components.

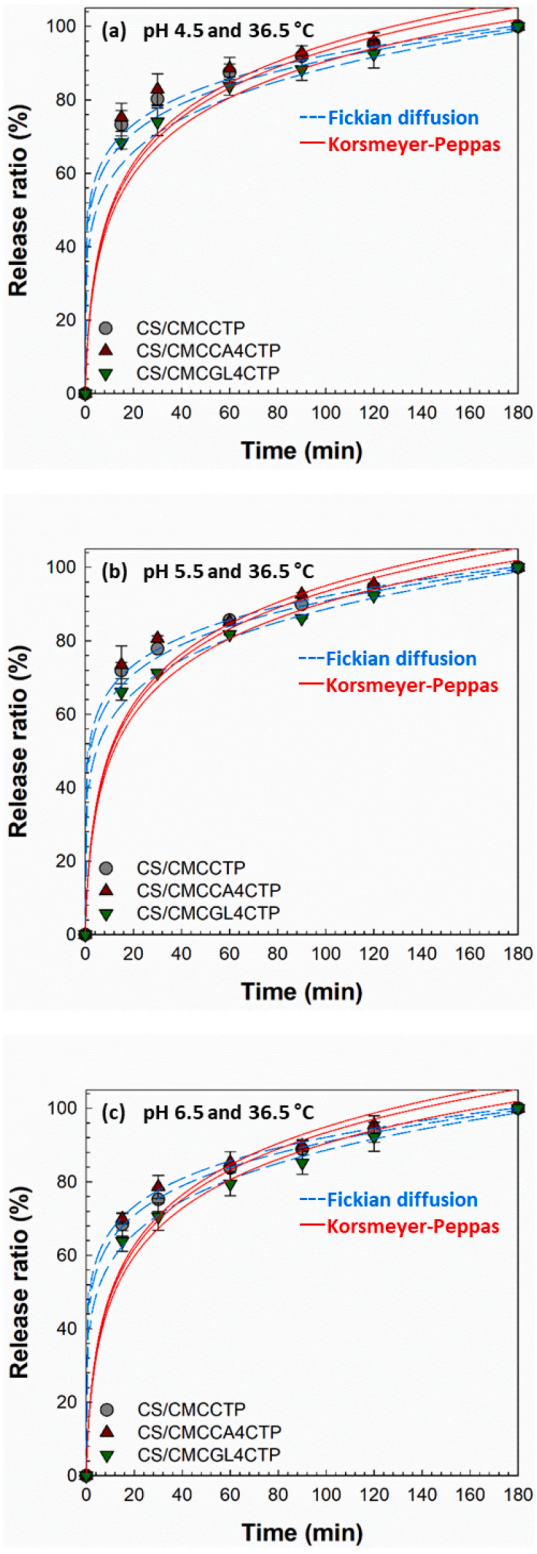

Fig. 4. CTP release behavior and mathematical model regression with various pH buffers at 36.5 °C. (a) CTP release from CTP-incorporated biomaterials with/without the addition of plasticizer at pH 4.5. (b) CTP release from CTP-incorporated biomaterials with/without the addition of plasticizer at pH 5.5. (c) CTP release from CTP-incorporated biomaterials with/without the addition of plasticizer at pH 6.5.

3.2. CTP release properties

The drug release profiles from CTP-incorporated CS/CMC biomaterials were obtained to establish their applicability for a TDDS. Fig. 4 shows CTP release behavior and UV absorbance curves from the CTP-incorporated biomaterials with/without plasticizers in release media with various pH at 36.5 °C. The CTP was rapidly released in the first 90 min and subsequently completely released in 180 min. CTP release ratio (%) was significantly different according to the plasticizer added to the biomaterial in the following order: CS/CMCCA4CTP > CS/CMCCTP > CS/CMCGL4CTP. The results follow the water resistance properties of the prepared CS/CMC biomaterials (see Fig. 1b). Nematollahi et.al [53] and Kuo et.al [54] have reported that the water resistance properties are an important factor in the determination of the diffusion rate of drugs in a matrix into the release medium. From the results, it can be seen that CTP release was the fastest in CA-added biomaterials with the highest WU and S values and the slowest in GL-added biomaterials with the lowest WU and S values. In addition, the pH value of the release medium affected the CTP release behavior. The CTP release ratio (%) at low pH levels was higher than at high pH levels because more free proton ions present at low pH can weaken the interactions between the carboxyl groups of CMC and the amine groups of CS. Thus, the drug from the biomaterials is readily diffused into the release medium accordingly. However, the number of protons is reduced at high pH, thus the electrostatic interactions between CS and CMC are stronger. Hence, the polymer network structure is compact and CTP is released relatively slowly from CTP-incorporated biomaterials [55]. UV absorbance curves for CTP release over time from CTP-incorporated biomaterials with/without the addition of plasticizers (CA and GL) at different pH values (pH 4.5, pH 5.5, and pH 6.5) and 36.5 °C are shown in Fig. S1. It can be seen that the absorbance peak at 200.0 nm (the characteristic peak for CTP) increased with an increase in release time. This increasing tendency was evidenced by the rapid release of CTP from manufactured biomaterials into the buffer at 15 min and near equilibrium at 120 min.

Mathematical modeling is commonly used in various fields, such as genetics, medicine, and engineering. Especially, it can be useful for predicting drug release kinetics and designing controlled drug release formulations. The models can be fitted by measuring parameters such as drug diffusion coefficients and experimental data, etc. In the present study, we utilized two diffusion models (Fickian diffusion and Korsmeyer-Peppas models) to evaluate the most likely drug diffusion mechanism for CTP release.

Fig. 4 and Table 2 provide the results of applying mathematical models to the CTP release profiles of the prepared CTP-incorporated CS/CMC biomaterials in various pH buffer solutions at 36.5 °C. These results indicate that the Fickian diffusion model (the dashed line) is more suitable than the Korsmeyer-Peppas model (the solid line). The diffusion coefficient (D_{eff}) values of CS/CMCGL4CTP were lower than those of CS/CMCCTP whereas those of CS/CMCCA4CTP were higher. In addition, the D_{eff} values increased with decreasing pH values. CTP release from CS/CMCCA4CTP at pH 4.5 provided the highest D_{eff} value (8.190E-11), which is 1.97 times higher than that of CTP release from CS/CMCGL4CTP at pH 6.5 (4.675E-11; the lowest D_{eff} value). The results using the Korsmeyer-Peppas model confirm that the prepared CTP-incorporated biomaterials have diffusional exponents (n) of <0.5, which unambiguously verifies that the CTP release profiles of the prepared biomaterials at various pH values follow the pseudo-Fickian diffusion mechanism.

RSM analysis with the changes of pH value and temperature was conducted to investigate optimal CTP release from the biomaterials. The effects of pH and temperature on the CTP release ratio (%) from CTP-incorporated biomaterials with/without plasticizers (CA and GL) at CTP release time of 30.0 min are shown in Fig. 5. Results indicate that CTP release at low pH levels and high temperatures was higher than at high pH levels and low temperatures. From the results, in the case of the CTP release from CTP-incorporated biomaterials without the addition of

Table 2
Fickian diffusion and Korsmeyer-Peppas model parameters of CTP release from CTP-incorporated CS/CMC biomaterials using various pH buffers.

	CS/CMCCTP			CS/CMCCA4CTP			CS/CMCGL4CTP		
Fickian diffusion model									
pH	4.5	5.5	6.5	4.5	5.5	6.5	4.5	5.5	6.5
M_∞	100.207	100.202	100.347	100.225	100.178	100.182	100.344	100.346	100.348
D_{eff}	8.190 E-11	7.339 E-11	6.206 E-11	9.225 E-11	8.261 E-11	7.186 E-11	6.118 E-11	5.133 E-11	4.675 E-11
R^2	1.000	0.999	0.999	0.999	0.999	0.999	0.999	0.998	0.998
Korsmeyer-Peppas model									
pH	4.5	5.5	6.5	4.5	5.5	6.5	4.5	5.5	6.5
M_∞	526.994	516.427	495.638	510.575	526.458	508.401	494.582	476.824	464.204
k	0.0099	0.0091	0.0090	0.0104	0.0096	0.0094	0.0090	0.0085	0.0081
n	0.125	0.147	0.154	0.112	0.134	0.142	0.115	0.172	0.185
R^2	0.823	0.825	0.862	0.879	0.847	0.894	0.895	0.833	0.859

the plasticizers (CS/CMCCTP), the maximum CTP release ratio (%) was 81.0021 % at pH 4.75 and 40.0 °C (see Fig. 5a). The maximum CTP release ratio (%) of CS/CMCCA4CTP (see Fig. 5b), and CS/CMCGL4CTP (see Fig. 5c) was 84.7326 % (pH 4.5 and 40.0 °C), and 78.0671 % (pH 4.5 and 40.0 °C), respectively. As a result, the maximum CTP release could be verified in CA-added CTP-incorporated biomaterial (CS/CMCCA4CTP). As mentioned, results for CTP release, it could be reconfirmed that the CTP release from CA-added CTP-incorporated biomaterial was the fastest compared to other biomaterials.

3.3. CTP release properties using an artificial skin test

To identify the applicability of the CTP-incorporated biomaterials as a TDDS for antihypertensive therapy, CTP release properties were evaluated using an artificial skin test. Fig. 6a shows the CTP release behavior of the prepared biomaterials with/without plasticizers using artificial skin at 36.5 °C and RH 60 %. The results confirm that CTP was constantly released from the prepared biomaterials for 36 h. Moreover, the degree of CTP release fluctuated according to the type of plasticizers, which is a similar trend to the results of CTP release into various pH buffers. As mentioned above, various oral formulations have been reported to control the release of CTP [17–19]. The CTP-incorporated CS/CMC biomaterials prepared in this study sustained CTP release more effectively than these biomaterials for oral administration. Additionally, while the release of other drugs using the CS/CMC complex indicated burst drug release in the initial time, the prepared CS/CMC biomaterials were released relatively slowly in the artificial skin model [30,55]. Therefore, the sustained and slow drug release of the prepared CS/CMC biomaterials is considered suitable for long-term treatment of chronic diseases such as hypertension. Mathematical models were applied to determine the mechanism of CTP release through the artificial skin (Fig. 6 and Table 3). The estimated D_{eff} values for CTP release properties show that it fitted the Fickian diffusion model: CS/CMCCA4CTP; 8.963E-12 > CS/CMCCTP; 8.526E-12 > CS/CMCGL4CTP; 6.876E-12. The R^2 values for the mathematical models indicate that CTP release can be better explained by the Korsmeyer-Peppas model than by the Fickian diffusion model. In addition, the n values for CTP release obtained from the Korsmeyer-Peppas model were between 0.51 and 0.63; since the n values of the CTP-incorporated biomaterials with/without the addition of plasticizers exceeded 0.5, the CTP release properties using the artificial skin followed a non-Fickian diffusion mechanism.

Fig. 6b shows the results of CTP release (%) for CTP-incorporated biomaterials with/without the addition of PN. Results revealed that CTP release was increased about 1.12–1.32 times by the addition of PN. In addition, it could be verified that the degree of CTP release was improved by the number of PN added to CTP-incorporated biomaterials because the CTP release rate was increased with increasing of the number of PN. The reason is that the CTP was effectively diffused in the skin because of the penetration of PN into the skin. Thus, results suggest that PN used in oriental medicine on biomaterials for a TDDS patch could be helpful for improving the effects of therapy and designing a controlled release of the drug.

Thermogravimetric analysis (TGA) and differential scanning calorimetry (DSC) of CTP and prepared CTP-incorporated CS/CMC biomaterials before/after CTP release was shown in Fig. 7. Fig. 7a shows the results of TGA curves of CTP and CS/CMC biomaterials with/without incorporating CTP and before/after CTP release. From the results of TGA of CTP, it could be clearly confirmed that weight loss (%) occurred at 252.0 °C. In addition, about 95 % weight loss was observed between 252.0 and 400.0 °C. This result was found to be similar to the study reported by Tayyab et al. [56]. Benghanem et al. [57] and Zhu et al. [58] have reported that the thermal decomposition of CS/CMC biomaterials occurred in the range of 100–560 °C with a total mass loss of about 62.0 %. The same results were obtained in this study for CS/CMC biomaterial without the addition of CTP. Results of TGA analysis of CS/CMC biomaterial with/without incorporating CTP indicated that the TGA curve of CTP-incorporated CS/CMC biomaterial shifted the high temperature region. It means that the thermal properties are slightly improved by the addition toward of CTP. However, after CTP release, the TGA curve of CTP-released CS/CMC biomaterial was lower than that of others. The results suggest that CTP-incorporated in CS/CMC biomaterial was released and network structures of biomaterial were slightly modified by the release of CTP. In addition, we confirmed that CTP was released above 95.0 % by weight loss. Fig. 7b shows the results of thermal properties of CA or GL-added CTP-incorporated CS/CMC biomaterials before/after CTP release. Results indicated that TGA curves of CA or GL-added CTP-incorporated CS/CMC biomaterials shifted the low temperature region compared to CS/CMC biomaterials without the addition of CA and GL as plasticizers. The phenomenon is because plasticizers are relatively sensitive to thermal decomposition. From the results of TGA of CA or GL-added CTP-incorporated CS/CMC biomaterials before/after CTP release, it could be verified that TGA curves of CTP released CS/CMC biomaterials with the addition of plasticizers were lowered because of CTP release. Fig. 7c shows the results of DSC curves of CTP and CS/CMC biomaterials with/without incorporating CTP and before/after CTP release. The strong endothermic peak at 108.93 °C (ΔH = 118.9 J/g) is related to the melting point of the CTP [56]. Endothermic peaks were observed at 115.53 °C (ΔH = 318.1 J/g) and 116.15 °C (ΔH = 379.7 J/g) for CS/CMC biomaterials and CTP-incorporated CS/CMC biomaterials, respectively. The variation in the ΔH of these endothermic reactions indicates a change in the interaction and thermal properties of the biomaterials due to CTP loading [59]. Furthermore, the exothermic peak at 265–330 °C is attributed to the degradation of CS/CMC biomaterials [60]. The DSC curve of the CS/CMC biomaterials after CTP release shows an endothermic peak at 87.88 °C (ΔH = 308.0 J/g) and an exothermic peak at 269.26 °C (ΔH = 223.5 J/g). These shifted peaks are due to the deformation induced in the network of the biomaterials by the release of CTP. The DSC thermogram in Fig. 7d represents the results of CA or GL-added CTP-incorporated CS/CMC biomaterials before/after CTP release. CA or GL-added

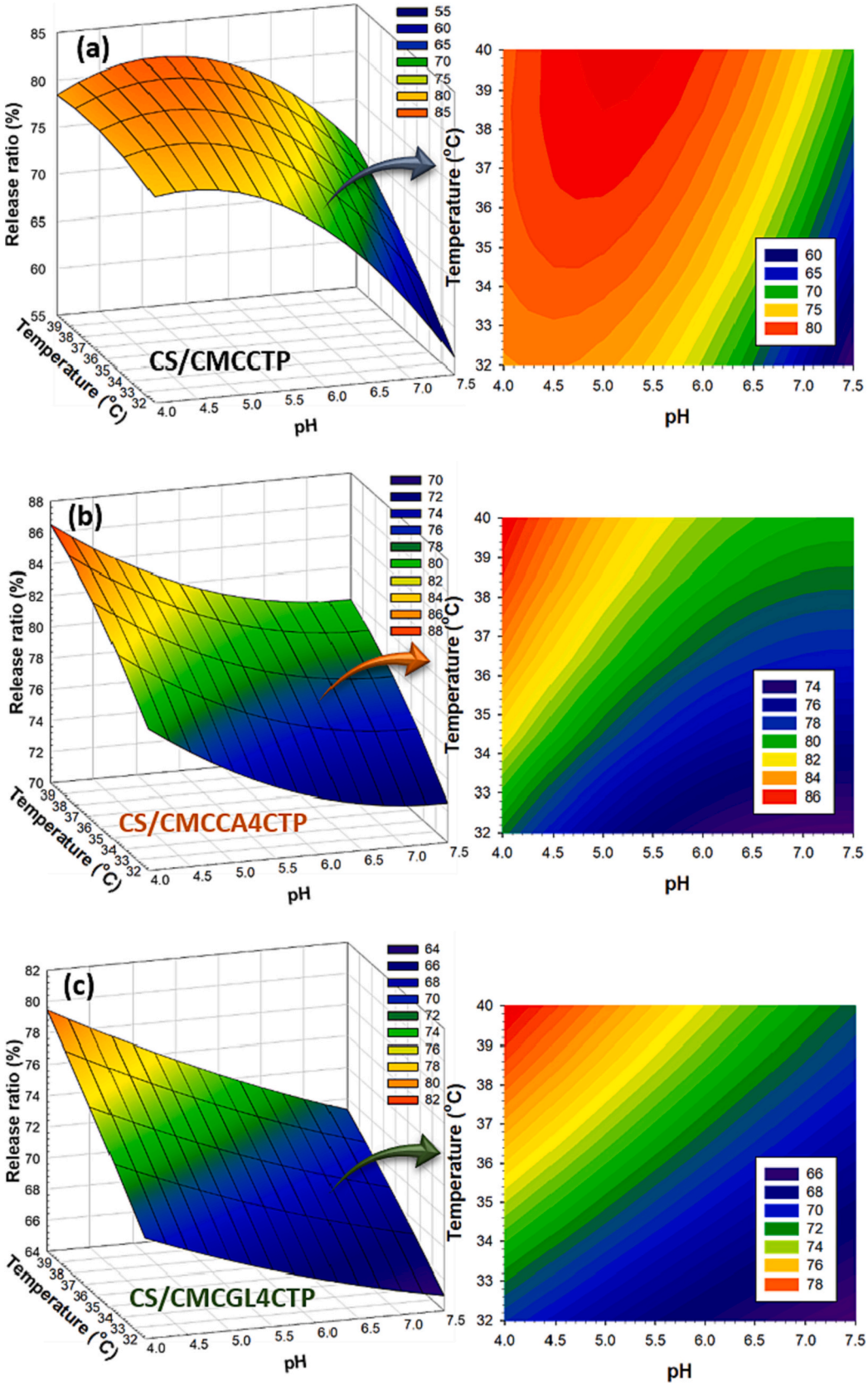

Fig. 5. Effect of pH and temperature factors on the release ratio (%). (a) CTP-incorporated CS/CMC biomaterials. (b) CTP-incorporated CS/CMC biomaterials with CA. (c) CTP-incorporated CS/CMC biomaterials with GL.

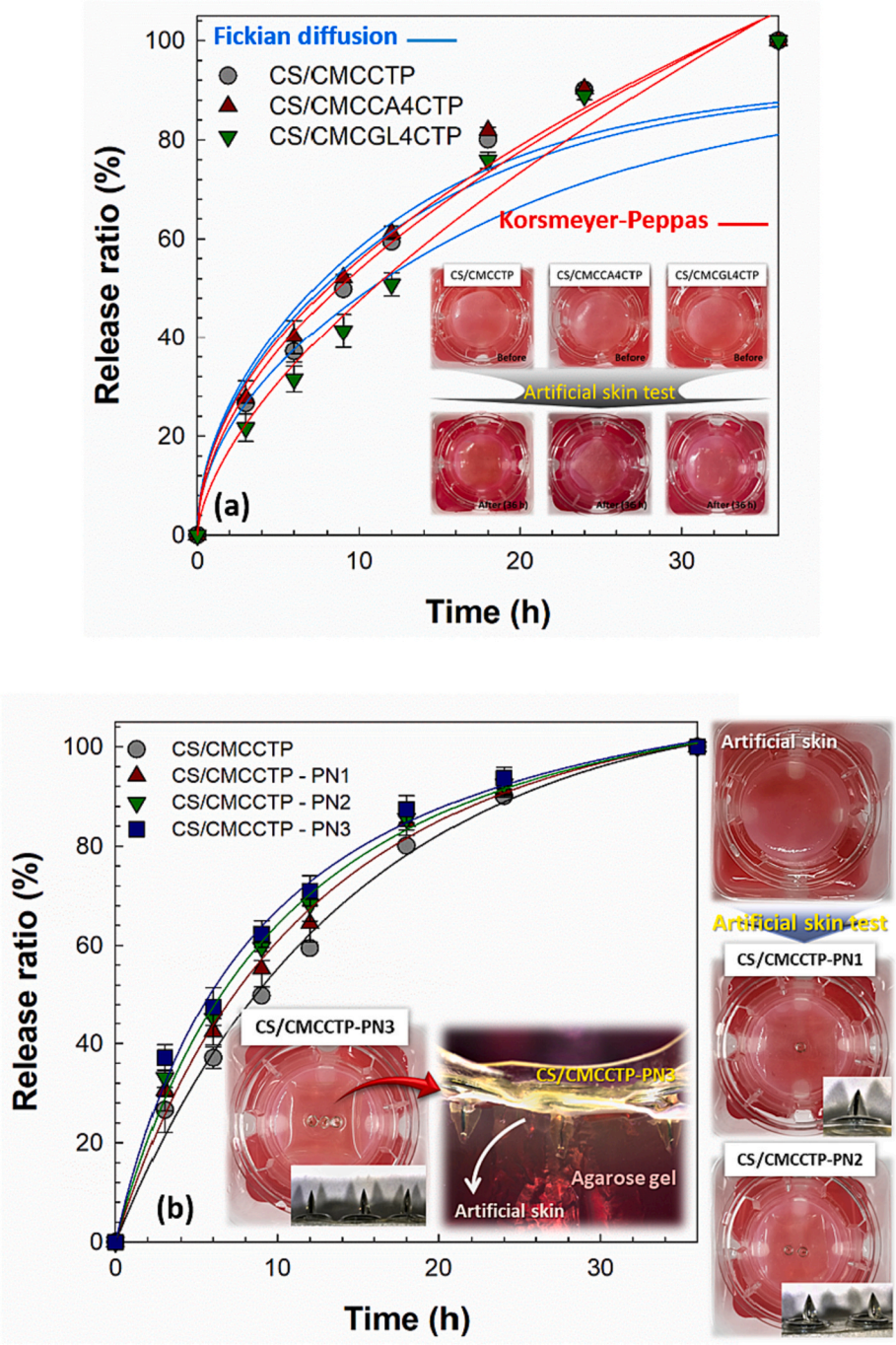

Fig. 6. CTP release behavior using artificial skin test at 36.5 °C and RH 60 %. (a) Experimental and Fickian diffusion and Korsmeyer-Peppas model fitting of CTP release from CTP-incorporated biomaterials with/without the addition of plasticizer. (b) CTP release ratio (%) from CTP-incorporated biomaterials added with press needles.

CTP-incorporated CS/CMC biomaterials exhibited endothermic peaks in the low temperature region below 100 °C compared to biomaterials without the addition of plasticizers. These results are attributed to the evaporation of water and the degradation of plasticizers. In the case of CTP release, the DSC curves of CA or GL-added biomaterials showed similar results to those of non-added biomaterials because of the solubility of the plasticizers and the release of CTP inside the biomaterials.

3.4. ACE inhibition by the CTP-incorporated biomaterials

Since ACE inhibitors are widely used in antihypertensive therapy [61], we investigated ACE inhibition by the CTP-incorporated biomaterials with/without the addition of plasticizers for potential use in antihypertensive treatment. Fig. 8a–c shows the absorbance measurements at 228 nm for each group. The absorbance of the C and D groups was measured using a reaction stopping solution to eliminate the absorbance error of the A and B groups. Fig. 8d presents the ACE inhibition results of the released CTP from the prepared biomaterials with reaction time. Interestingly, not only CTP-incorporated biomaterials but also the biomaterials without the addition of CTP effectively inhibited ACE. In particular, plasticizers-added biomaterials showed relatively high ACE inhibition, which can be attributed to the various functional groups in the plasticizers. Previously, it has been reported that the hydroxyl and carboxyl groups can bind to the active site of ACE via

Table 3
Fickian diffusion and Korsmeyer-Peppas model parameters of CTP release from CTP-incorporated CS/CMC biomaterials through artificial skin tests.

	CS/CMCCTP	CS/CMCCA4CTP	CS/CMCGL4CTP
Fickian diffusion model			
M_∞	104.705	104.804	104.389
D_{eff}	8.526 E-12	8.963E-12	6.876E-12
R^2	0.873	0.880	0.836
Korsmeyer-Peppas model			
M_∞	107.696	102.219	102.536
k	0.136	0.144	0.110
n	0.528	0.510	0.627
R^2	0.985	0.985	0.982

intermolecular interactions [62]. Thus, since the functional groups in the CS/CMC complex are capable of inter-intramolecular interactions, the complex could effectively inhibit ACE. Moreover, the ACE inhibitory activities depended on the type of plasticizers added to the biomaterials, with the activities being in the following order: CS/CMCCA4CTP > CS/CMCGL4CTP > CS/CMCCTP. CS/CMCCA4CTP had the highest ACE inhibition activity (88.44 %), which was 1.11 times higher than that of CS/CMCCTP (79.74 %), which suggests that the functional groups in CA enhanced ACE inhibition.

4. Conclusions

CTP-incorporated biomaterials comprising CS, CMC, and plasticizers (CA and GL) were successfully prepared using a casting method followed by a UV curing process. An optimal UV irradiation time of 40 min was confirmed by examining the water resistance properties of the resulting complexes. The stability of CTP with/without the biomaterials was unaffected by the preparation process, as confirmed by using UV–vis, FT-IR, and ^{1}H NMR spectroscopy. The chemical structure and morphology of the prepared biomaterials were characterized using FE-SEM and FT-IR analysis. CTP was released from CTP-incorporated

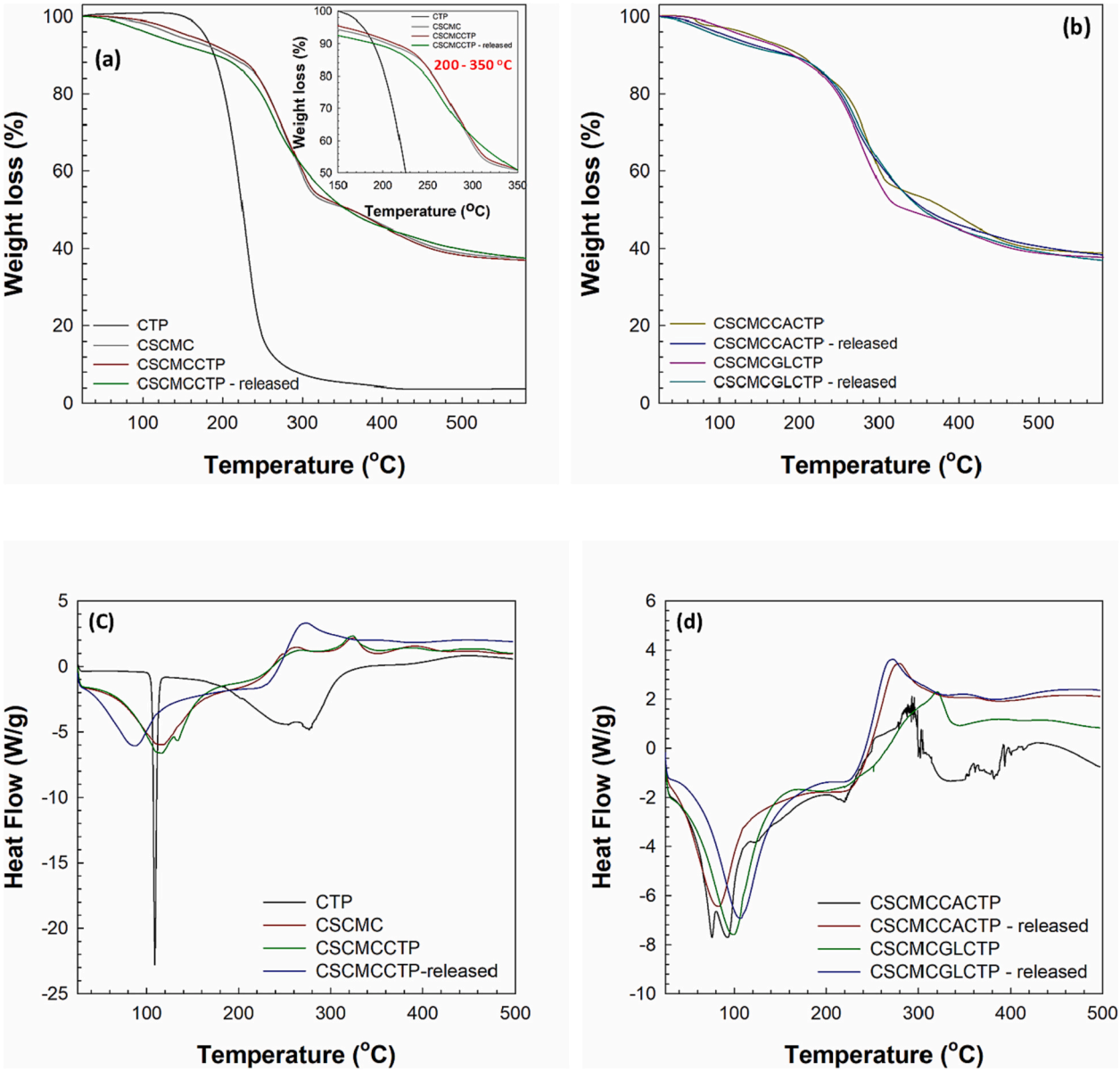

Fig. 7. TGA and DSC of the prepared CS/CMC biomaterials. (a) TGA curves of CTP and CS/CMC biomaterials with/without the addition of CTP and before/after CTP release. (b) TGA curves of CA or GL-added CTP-incorporated CS/CMC biomaterials before/after CTP release. (c) DSC curves of CTP and CS/CMC biomaterials with/without the addition of CTP and before/after CTP release. (d) DSC curves of CA or GL-added CTP-incorporated CS/CMC biomaterials before/after CTP release.

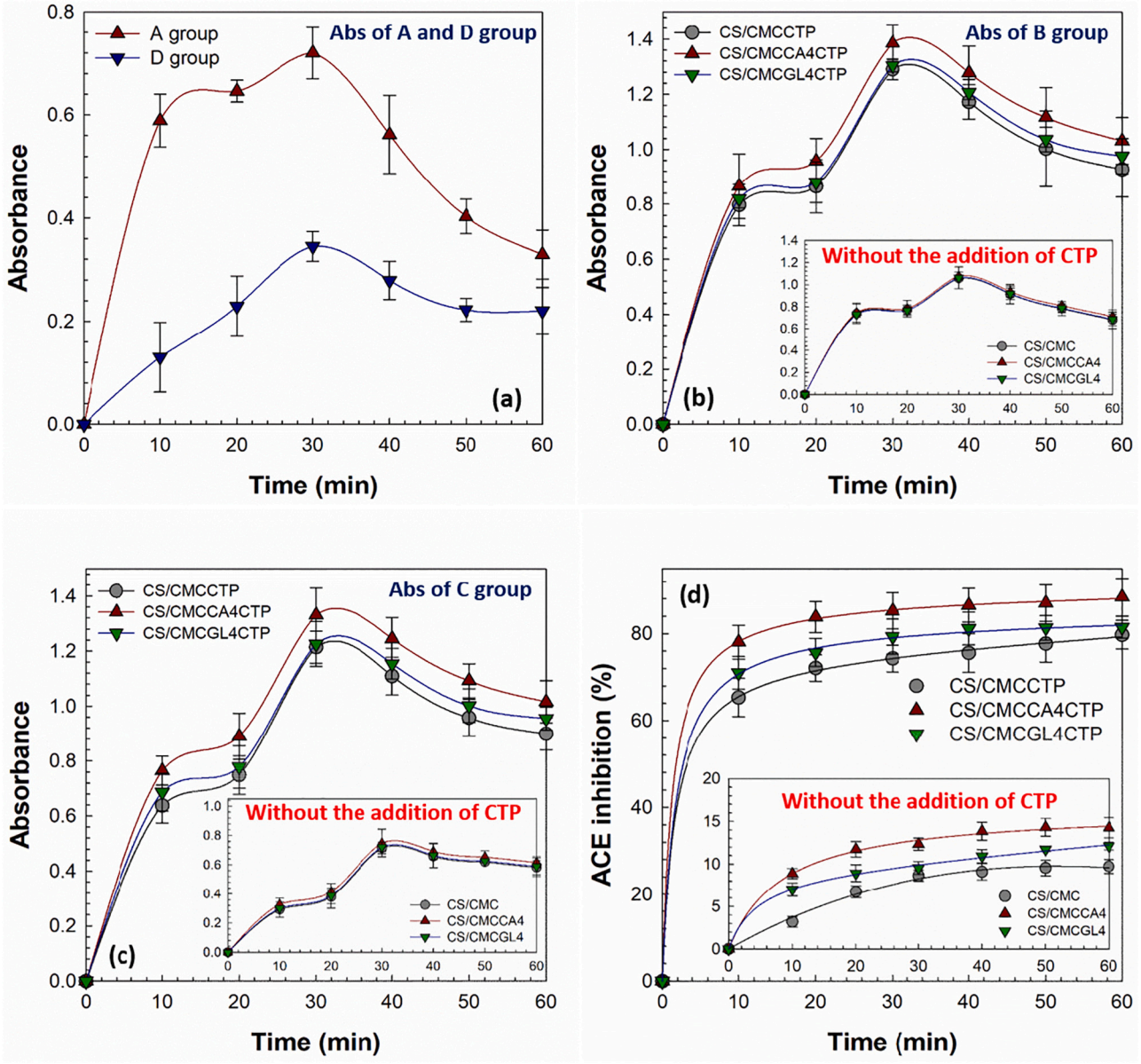

Fig. 8. ACE inhibitory activities of CS/CMC biomaterials with/without CTP and plasticizers. (a) UV absorbance at 228 nm of A and D groups. (b) UV absorbance at 228 nm of B group. (c) UV absorbance at 228 nm of C group. (d) ACE inhibition (%) of CS/CMC biomaterials with/without CTP and plasticizers.

biomaterials into buffers of various pH values and at various temperatures within 180 min. The CTP release rate at low pH and high temperature was higher than that at high pH and low temperature. In addition, the CTP release rate was significantly affected by the type of plasticizers added to the biomaterial. To assess the applicability of the prepared biomaterials for use as a TDDS, CTP release profiles were attained via artificial skin tests at 36.5 °C and RH 60 %. The results exhibited that CTP was continuously released from the prepared biomaterials within 36 h. In addition, CTP release from CA-added biomaterials was around 1.30 times higher than that from GL-added biomaterials. Results revealed that the CTP release of CTP-incorporated biomaterials combined press needles was 1.12–1.32 times higher than that of CTP-incorporated biomaterial without the addition of press needles. Mathematical modeling shows that the CTP release mechanism follows a pseudo-Fickian diffusion mechanism in the buffer medium and a non-Fickian diffusion mechanism in the artificial skin model. The results of the ACE inhibitory activity for the prepared biomaterials revealed that CTP-incorporated biomaterials effectively inhibited ACE and that CA and GL as plasticizers added to the biomaterials had a positive effect on ACE inhibitory activities. Thus, the prepared CTP-incorporated CS/CMC biomaterials could be applied as a TDDS for antihypertensive treatment.

Supplementary data to this article can be found online at https://doi.org/10.1016/j.ijbiomac.2023.128087.

CRediT authorship contribution statement

Kyeong-Jung Kim: Conceptualization, Methodology, Validation, Formal analysis, Resources, Data curation, Writing – original draft, Visualization. **Min-Jin Hwang:** Conceptualization, Software, Formal analysis, Data curation. **Wang-Geun Shim:** Conceptualization, Methodology, Software, Formal analysis. **Young-Nam Youn:** Conceptualization, Methodology, Software, Formal analysis, Resources, Writing – original draft, Visualization. **Soon-Do Yoon:** Conceptualization, Methodology, Software, Validation, Formal analysis, Resources, Data curation, Writing – original draft, Visualization.

Declaration of competing interest

The authors declare that they have no known competing financial interests or personal relationships that could have appeared to influence the work reported in this paper.

Acknowledgment

This research was supported by Basic Science Research Program through the National Research Foundation of Korea (NRF) funded by the Ministry of Education (Grant no. NRF-2019R1I1A3A01061508).

References

[1] R. Diab, C.J. Maalej, H. Fessi, P. Maincent, Engineered nanoparticulate drug delivery systems: the next frontier for oral administration? AAPS J. 14 (2012) 688–702, https://doi.org/10.1208/s12248-012-9377-y.
[2] E. Roger, F. Lagarce, E. Garcion, J.P. Benoit, Biopharmaceutical parameters to consider in order to alter the fate of nanocarriers after oral delivery, Nanomedicine-UK. 5 (2010) 287–306, https://doi.org/10.2217/nnm.09.110.
[3] M.R. Prausnitz, R. Langer, Transdermal drug delivery, Nat. Biotechnol. 26 (2008) 1261–1268, https://doi.org/10.1038/nbt.1504.
[4] M.K. Malaiya, A. Jain, H. Pooja, A. Jain, D. Jain, Controlled delivery of rivastigmine using transdermal patch for effective management of Alzheimer's disease, J. Drug Deliv. Sci. Technol. 45 (2018) 408–414, https://doi.org/10.1016/j.jddst.2018.03.030.
[5] M.R. Prausnitz, S. Mitragotri, R. Langer, Current status and future potential of transdermal drug delivery, Nat. Rev. Drug Discov. 3 (2004) 115–124, https://doi.org/10.1038/nrd1304.
[6] A.H. Sabri, J. Ogilvie, K. Abdulhamid, V. Shpadaruk, J. Mckenna, J. Segal, D. J. Scurr, M. Marlow, Expanding the applications of microneedles in dermatology, Eur. J. Pharm. Biopharm. 140 (2019) 121–140, https://doi.org/10.1016/j.ejpb.2019.05.001.
[7] B.M. Egan, S.E. Kjeldsen, G. Grassi, M. Esler, G. Mancia, The global burden of hypertension exceeds 1.4 billion people: should a systolic blood pressure target below 130 become the universal standard? J. Hypertens. 37 (2019) 1148–1153, https://doi.org/10.1097/HJH.0000000000002021.
[8] K.T. Mills, A. Stefanescu, J. He, The global epidemiology of hypertension, Nat. Rev. Nephrol. 16 (2020) 223–237, https://doi.org/10.1038/s41581-019-0244-2.
[9] F.D. Fuchs, P.K. Whelton, High blood pressure and cardiovascular disease, Hypertension 75 (2020) 285–292, https://doi.org/10.1161/HYPERTENSIONAHA.119.14240.
[10] Z. Zeng, J. Chen, C. Xiao, W. Chen, A global view on prevalence of hypertension and human develop index, Ann. Glob. Health 86 (2020) 67, https://doi.org/10.5334/aogh.2591.
[11] M.R. Cunha, E.C. Lima, D.R. Lima, R.S.D. Silva, P.S. Thue, M.K. Seliem, F. Sher, G. S.D. Reis, S.H. Larsson, Removal of captopril pharmaceutical from synthetic pharmaceutical-industry wastewaters: use of activated carbon derived from Butia catarinensis, J. Environ. Chem. Eng. 8 (2020), 104506, https://doi.org/10.1016/j.jece.2020.104506.
[12] G.H. Li, H. Liu, Y.H. Shi, G.W. Le, Direct spectrophotometric measurement of angiotensin I-converting enzyme inhibitory activity for screening bioactive peptides, J. Pharm. Biomed. 37 (2005) 219–224, https://doi.org/10.1016/j.jpba.2004.11.004.
[13] J. Wu, R.E. Aluko, A.D. Muir, Improved method for direct high-performance liquid chromatography assay of angiotensin-converting enzyme-catalyzed reactions, J. Chromatogr. A 950 (2002) 125–130, https://doi.org/10.1016/S0021-9673(02)00052-3.
[14] I. Fleming, Signaling by the angiotensin-converting enzyme, Circ. Res. 98 (2006) 887–896, https://doi.org/10.1161/01.RES.0000217340.40936.53.
[15] R. Gugler, H. Allgayer, Effects of antacids on the clinical pharmacokinetics of drugs: an update, Clin. Pharmacokinet. 18 (1990) 210–219, https://doi.org/10.2165/00003088-199018030-00003.
[16] K.L. Duchin, D.N. Mckinstry, A.I. Cohen, B.H. Migdalof, Pharmacokinetics of captopril in healthy subjects and in patients with cardiovascular diseases, Clin. Pharmacokinet. 14 (1988) 241–259, https://doi.org/10.2165/00003088-198814040-00002.
[17] Y. Ikeda, K. Kimura, F. Hirayama, H. Arima, K. Uekama, Controlled release of a water-soluble drug, captopril, by a combination of hydrophilic and hydrophobic cyclodextrin derivatives, J. Control. Release 66 (2000) 271–280, https://doi.org/10.1016/S0168-3659(99)00286-2.
[18] H.K. Stulzer, M.A.S. Silva, D. Fernades, J. Assreuy, Development of controlled release captopril granules coated with ethylcellulose and methylcellulose by fluid bed dryer, Drug Deliv. 15 (2008) 11–18, https://doi.org/10.1080/10717540701827196.
[19] S. Yimin, C. Xiguangm T, L. Chengshen Xuexi, M. Xianghong, Y. Luojun, Preparation and characterization in vitro of sustained-release captopril/chitosan-gelatin net-polymer microspheres (Cap/CGNPMs), J. Wuhan Univ. Technol. Mater. Sci. Ed. 21 (2006) 35–40, https://doi.org/10.1007/BF02840875.
[20] M.H. Weinberger, Comparison of captopril and hydrochlorothiazide alone and in combination in mild to moderate essential hypertension, Br. J. Clin. Pharmacol. 14 (1982) 127S–131S, https://doi.org/10.1111/j.1365-2125.1982.tb02069.x.
[21] H. Zaher, H. Rasheed, M.M.E. Komy, R.A. Hegazy, H.I. Gawdat, D.M.A. Halim, R. M.A. Hay, R.A. Hegazy, A.M. Mohy, Propranolol versus captopril in the treatment of infantile hemangioma (IH): a randomized controlled trial, J. Am. Acad. Dermatol. 74 (2016) 499–505, https://doi.org/10.1016/j.jaad.2015.09.061.
[22] F. Croisier, C. Jérôme, Chitosan-based biomaterials for tissue engineering, Eur. Polym. J. 49 (2013) 780–792, https://doi.org/10.1016/j.eurpolymj.2012.12.009.
[23] N.M. Crini, E. Lichtfouse, G. Torri, G. Crini, Applications of chitosan in food, pharmaceuticals, medicine, cosmetics, agriculture, textiles, pulp and paper, biotechnology, and environmental chemistry, Environ. Chem. Lett. 17 (2019) 1667–1692, https://doi.org/10.1007/s10311-019-00904-x.
[24] A. Pettignano, A. Charlot, E. Fleury, Carboxyl-functionalized derivatives of carboxymethyl cellulose: towards advanced biomedical applications, Polym. Rev. 59 (2019) 510–560, https://doi.org/10.1080/15583724.2019.1579226.
[25] S. Javanbakht, A. Shaabani, Carboxymethyl cellulose-based oral delivery systems, Int. J. Biol. Macromol. 133 (2019) 21–29, https://doi.org/10.1016/j.ijbiomac.2019.04.079.
[26] V.F. Lotfy, S.S. Hassan, P.A.K. Alla, The role of side chain of amino acid on performance of their conjugates with carboxymethyl cellulose and their Pd(II) complexes as bioactive agents, Int. J. Polym. Mater. 69 (2020) 21–31, https://doi.org/10.1080/00914037.2019.1670179.
[27] A.H. Basta, V.F. Lotfy, K. Mahmoud, N.A.M. Abdelwahed, Synthesis and evaluation of protein-based biopolymer in production of silver nanoparticles as bioactive compound versus carbohydrates-based biopolymers, R. Soc. Open Sci. 7 (2020), 200928, https://doi.org/10.1098/rsos.200928.
[28] A.H. Basta, V.F. Lotfy, C. Eldewany, Comparison of copper-crosslinked carboxymethyl cellulose versus biopolymer-based hydrogels for controlled release of fertilizer, Polym.-Plast. Tech. Mater. 60 (2021) 1884–1897, https://doi.org/10.1080/25740881.2021.1934017.
[29] Y. Wang, F. Tang, J. Xia, T. Yu, J. Wang, R. Azhati, X.D. Zheng, A combination of marine yeast and food additive enhances preventive effects on postharvest decay of jujubes (*Zizyphus jujuba*), Food Chem. 125 (2011) 835–840, https://doi.org/10.1016/j.foodchem.2010.09.032.
[30] F. Wang, Q. Zhang, X. Li, K. Huang, W. Shao, D. Yao, C. Huang, Redox-responsive blend hydrogel films based on carboxymethyl cellulose/chitosan microspheres as dual delivery carrier, Int. J. Biol. Macromol. 134 (2019) 413–421, https://doi.org/10.1016/j.ijbiomac.2019.05.049.
[31] C. Tu, R.D. Zhang, C. Yan, Y. Guo, L. Cui, A pH indicating carboxymethyl cellulose/chitosan sponge for visual monitoring of wound healing, Cellulose 26 (2019) 4541–4552, https://doi.org/10.1007/s10570-019-02378-0.
[32] J. Liuyun, L. Yubao, X. Chengdong, Preparation and biological properties of a novel composite scaffold of nano-hydroxyapatite/chitosan/carboxymethyl cellulose for bone tissue engineering, J. Biomed. Sci. 16 (2009) 1–10, https://doi.org/10.1186/1423-0127-16-65.
[33] M. Mohammadi, M.H. Azizi, A. Zoghi, Antimicrobial activity of carboxymethyl cellulose–gelatin film containing Dianthus barbatus essential oil against aflatoxin-producing molds, Food Sci. Nutr. 8 (2020) 1244–1253, https://doi.org/10.1002/fsn3.1413.
[34] A. Sionkowska, Current research on the blends of natural and synthetic polymers as new biomaterials, Prog. Polym. Sci. 36 (2011) 1254–1276, https://doi.org/10.1016/j.progpolymsci.2011.05.003.
[35] K.J. Kim, M.J. Hwang, Y.H. Yun, S.D. Yoon, Synthesis and drug release behavior of functional montelukast imprinted inulin-based biomaterials as asthma treatment, J. Ind. Eng. Chem. 109 (2022) 221–229, https://doi.org/10.1016/j.jiec.2022.02.003.
[36] M. Aqil, A. Ali, Monolithic matrix type transdermal drug delivery systems of pinacidil monohydrate: in vitro characterisation, Eur. J. Pharm. Biopharm. 54 (2002) 161–164, https://doi.org/10.1016/S0939-6411(02)00059-0.
[37] G.R. Qadri, A. Ahad, M. Aqil, S.S. Imam, A. Ali, Invasomes of isradipine for enhanced transdermal delivery against hypertension: formulation, characterization, and in vivo pharmacodynamic study, Artif. Cells Nanomed. Biotechnol. 45 (2017) 139–145, https://doi.org/10.3109/21691401.2016.1138486.
[38] Y.H. Yun, C.M. Lee, Y.S. Kim, S.D. Yoon, Preparation of chitosan/polyvinyl alcohol blended films containing sulfosuccinic acid as the crosslinking agent using UV curing process, Food Res. Int. 100 (2017) 377–386, https://doi.org/10.1016/j.foodres.2017.07.030.
[39] J.F. Rubilar, R.M.S. Cruz, R.N. Zuñiga, I. Khmelinskii, M.C. Vieira, Mathematical modeling of gallic acid release from chitosan films with grape seed extract and carvacrol, Int. J. Biol. Macromol. 104 (2017) 197–203, https://doi.org/10.1016/j.ijbiomac.2017.05.187.
[40] L.M. Marvdashti, M. Yavarmanesh, A. Koocheki, Controlled release of nisin from polyvinyl alcohol-Alyssum homolocarpum seed gum composite films: nisin kinetics, Food Biosci. 28 (2019) 133–139, https://doi.org/10.1016/j.fbio.2019.01.010.
[41] I.Y. Wu, S. Bala, N.Š. Basnet, M.P.D. Cagno, Interpreting non-linear drug diffusion data: utilizing Korsmeyer-Peppas model to study drug release from liposomes, Eur. J. Pharm. Sci. 138 (2019), 105026, https://doi.org/10.1016/j.ejps.2019.105026.
[42] J. Siepmann, N.A. Peppas, Modeling of drug release from delivery systems based on hydroxypropyl methylcellulose (HPMC), Adv. Drug Deliv. Rev. 64 (2012) 163–174, https://doi.org/10.1016/j.addr.2012.09.028.
[43] N. Malekjani, S.M. Jafari, Modeling the release of food bioactive ingredients from carriers/nanocarriers by the empirical, semiempirical, and mechanistic models, Compr. Rev. Food Sci. Food Saf. 20 (2021) 3–47, https://doi.org/10.1111/1541-4337.12660.
[44] S. Brahima, C. Boztepe, A. Kunkul, M. Yuceer, Modeling of drug release behavior of pH and temperature sensitive poly (NIPAAm-co-AAc) IPN hydrogels using response

surface methodology and artificial neural networks, Mater. Sci. Eng. C 75 (2017) 425–432, https://doi.org/10.1016/j.msec.2017.02.081.
[45] S.Y. Lee, Y.H. Yun, G. Ahn, S.D. Yoon, Preparation of niacinamide imprinted starch-based biomaterials for treating of hyperpigmentation, Int. J. Biol. Macromol. 232 (2023), 123382, https://doi.org/10.1016/j.ijbiomac.2023.123382.
[46] D.W. Cushman, H.S. Cheung, Spectrophotometric assay and properties of the angiotensin-converting enzyme of rabbit lung, Biochem. Pharmacol. 20 (1971) 1637–1648, https://doi.org/10.1016/0006-2952(71)90292-9.
[47] H.S. Kim, K.J. Kim, M.W. Lee, S.Y. Lee, Y.H. Yun, W.G. Shim, S.D. Yoon, Preparation and release properties of arbutin imprinted inulin/polyvinyl alcohol biomaterials, Int. J. Biol. Macromol. 161 (2020) 763–770, https://doi.org/10.1016/j.ijbiomac.2020.06.105.
[48] W.F. Lai, C. Hu, G. Deng, K.H. Lui, X. Wang, T.H. Tsoi, S. Wang, W.T. Wong, A biocompatible and easy-to-make polyelectrolyte dressing with tunable drug delivery properties for wound care, Int. J. Pharm. 566 (2019) 101–110, https://doi.org/10.1016/j.ijpharm.2019.05.045.
[49] H.A. Pawar, K.G. Lalitha, K. Ruckmani, Alginate beads of captopril using galactomannan containing Senna tora gum, guar gum and locust bean gum, Int. J. Biol. Macromol. 76 (2015) 119–131, https://doi.org/10.1016/j.ijbiomac.2015.02.026.
[50] H.K. Stulzer, P.O. Rodrigues, T.M. Cardoso, J.S.R. Matos, M.A.S. Silva, Compatibility studies between captopril and pharmaceutical excipients used in tablets formulations, J. Therm. Anal. Calorim. 91 (2008) 323–328, https://doi.org/10.1007/s10973-006-7935-1.
[51] M. Shimazaki, J. Hasegawa, K. Kan, K. Nomura, Y. Nose, H. Kondo, T. Ohashi, K. Watanabe, Synthesis of captopril starting from an optically active β-hydroxy acid, Chem. Pharm. Bull. 30 (1982) 3139–3146, https://doi.org/10.1248/cpb.30.3139.
[52] K. Chi, J.M. Catchmark, Improved eco-friendly barrier materials based on crystalline nanocellulose/chitosan/carboxymethyl cellulose polyelectrolyte complexes, Food Hydrocoll. 80 (2018) 195–205, https://doi.org/10.1016/j.foodhyd.2018.02.003.
[53] E. Nematollahi, M. Pourmadadi, F. Yazdian, H. Fatoorehchi, H. Rashedi, M. N. Nigjeh, Synthesis and characterization of chitosan/polyvinylpyrrolidone coated nanoporous γ-Alumina as a pH-sensitive carrier for controlled release of quercetin, Int. J. Biol. Macromol. 183 (2021) 600–613, https://doi.org/10.1016/j.ijbiomac.2021.04.160.
[54] C.Y. Kuo, Y.C. Wang, C.F. Lee, W.Y. Chiu, A novel route for preparation of multifunctional polymeric nanocarriers for stimuli-triggered drug release, J. Polym. Sci. A Polym. Chem. 52 (2014) 561–571, https://doi.org/10.1002/pola.27033.
[55] B. Cai, T. Zhong, P. Chen, J. Fu, Y. Jin, Y. Liu, R. Huang, L. Tan, Preparation, characterization and in vitro release study of drug-loaded sodium carboxymethylcellulose/chitosan composite sponge, PLoS One 13 (2018), e0206275, https://doi.org/10.1371/journal.pone.0206275.
[56] A. Tayyab, A. Mahmood, H. Ijaz, R.M. Sarfraz, N. Zafar, Z. Danish, Formulation and optimization of captopril-loaded microspheres based compressed tablets: in vitro evaluation, Int. J. Polym. Mater. 71 (2022) 233–245, https://doi.org/10.1080/00914037.2020.1825080.
[57] S. Benghanem, A. Chetouani, M. Elkolli, M. Bounekhel, D. Benachour, Grafting of oxidized carboxymethyl cellulose with hydrogen peroxide in presence of Cu(II) to chitosan and biological elucidation, Biocybern. Biomed. Eng. 37 (2017) 94–102, https://doi.org/10.1016/j.bbe.2016.09.003.
[58] H. Zhu, S. Chen, H. Duan, J. He, Y. Luo, Removal of anionic and cationic dyes using porous chitosan/carboxymethyl cellulose-PEG hydrogels: optimization, adsorption kinetics, isotherm and thermodynamics studies, Int. J. Biol. Macromol. 231 (2023), 123213, https://doi.org/10.1016/j.ijbiomac.2023.123213.
[59] V.F. Lotfy, A.H. Basta, Optimizing the chitosan-cellulose based drug delivery system for controlling the ciprofloxacin release versus organic/inorganic crosslinker, characterization and kinetic study, Int. J. Biol. Macromol. 165 (2020) 1496–1506, https://doi.org/10.1016/j.ijbiomac.2020.10.047.
[60] M.G. Burgaz, G. Torrado, S. Torrado, Characterization and superficial transformations on mini-matrices made of interpolymer complexes of chitosan and carboxymethylcellulose during in vitro clarithromycin release, Eur. J. Pharm. Biopharm. 73 (2009) 130–139, https://doi.org/10.1016/j.ejpb.2009.04.004.
[61] L. Hansson, L.H. Lindholm, L. Niskanen, J. Lanke, Y. Hedner, A. Niklason, K. Luomanmäki, B. Dahlöf, U.D. Faire, C. Mörlin, B.E. Karlberg, P.O. Wester, J. E. Björck, Effect of angiotensin-converting-enzyme inhibition compared with conventional therapy on cardiovascular morbidity and mortality in hypertension: the Captopril Prevention Project (CAPPP) randomised trial, Lancet 353 (1999) 611–616, https://doi.org/10.1016/S0140-6736(98)05012-0.
[62] N.A. Shukor, J.V. Camp, G.B. Gonzales, D. Staljanssens, K. Struijs, M.J. Zotti, K. Raes, G. Smagghe, Angiotensin-converting enzyme inhibitory effects by plant phenolic compounds: a study of structure activity relationships, J. Agric. Food Chem. 61 (2013) 11832–11839, https://doi.org/10.1021/jf404641v.